Journal of Hazardous Materials

Brazilian coal mining residues and sulphide oxidation by Fenton's reaction: An accelerated weathering procedure to evaluate possible environmental impact

L.F.O. Silva [a],[**], X. Querol [b], K.M. da Boit [a], S. Fdez-Ortiz de Vallejuelo [c], J.M. Madariaga [c],[*]

[a] Catarinense Institute of Environmental Research and Human Development – IPADHC, Capivari de Baixo, Santa Catarina, Brazil
[b] Institute of Environmental Assessment and Water Research (IDÆA-CSIC) C/Lluis Solé y Sabarís s/n, 08028 Barcelona, Spain
[c] Department of Analytical Chemistry, University of the Basque Country (EHU/UPV), P.O. Box 644, 48080 Bilbao, Basque Country, Spain

ARTICLE INFO

ABSTRACT

Fenton's reaction is proposed as an accelerated weathering test for sulphides associated with Brazilian Coal Mining Residues (CMR), that are exposed to oxygen and water during the mining of coal. TEM and SEM/EDX were used to evaluate the nature, occurrence and distribution of minerals in remaining coals and other lithological units, before and after applying the test. Oxidation of CMRs was examined by analyzing soluble sulphur (sulphate) and dissolved metals by ICP-MS or ICP OES. As dissolved sulphate increases, dissolved Zn, Cd, Cu and Co concentrations increase, leading to undetectable amounts in the remaining solid phases; dissolved Ni and Mn also increase with the mobilized sulphur, but the remainder in the solids is the most important fraction; Fe and Pb are not mobilized due to precipitation as jarosite or hematite in the case of Fe or as sulphate in the case of Pb. Agreement between the observed results and the predictions by geochemical modelling is discussed.

1. Introduction

Petroleum crises during the last few years have increased the significance of researching coal. Although abundant, existing coal reservoirs throughout the world could supply energy requirements for a long time, efficient use is limited by the coal's high sulphur content, as found in Brazilian coal, for example. The abundant presence of sulphide minerals associated with coal causes great concern as to the environmental impact of oxidation [1–4], together with the know CO_2 production after coal firing.

Significant environmental problems associated with coal mining arise from interaction between the sulphides from coal and the immediate environment, especially atmospheric compounds, surrounding surface and ground waters [5].

Most high-sulphur coals contain, among the different metal sulphides, high concentrations of pyritic sulphur. During the past two decades numerous studies have concentrated on understanding the mechanism of pyrite oxidation [6–10], due in part to the environmental impact of acid mine drainage [11–13]. Pyrite oxidation is an electrochemical process that consists of three distinct steps: (a) cathodic reaction, (b) electron transport and (c) anodic reaction [9].

Two chemical reactions are responsible for the first oxidation step: (a) aqueous pyrite oxidation by O_2, represented by the following overall reactions:

$$2FeS_2 + 7O_2 + 2H_2O \rightarrow 2Fe^{2+} + 4SO_4^{2-} + 4H^+ \qquad (1)$$
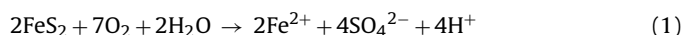
and (b) the own Ferric iron (Fe^{3+}), itself a powerful oxidant of pyrite in highly acidic conditions [13], which reacts with pyrite according to the following reaction:

$$FeS_2 + 14Fe^{3+} + 8H_2O \rightarrow 15Fe^{2+} + 2SO_4^{2-} + 16H^+ \qquad (2)$$
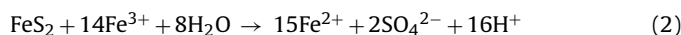
This cathodic reaction (the predominant one, (1) or (2), depends on the concentration of O_2 and Fe^{3+}) is the rate-determining step for sulphide mineral oxidation [10]. It oxidizes the sulphide to sulphate but maintains the iron in a state of ferrous oxidation. Studies on the oxidation of galena, sphalerite, chalcopyrite and arsenopyrite [9] concluded that the cathodic reaction (1) "is also true for these minerals, and is likely to be generally true".

Then, the ferrous iron (Fe^{2+}) released into solution is chemically oxidized to ferric iron by the dissolved oxygen:

$$Fe^{2+} + O_2 + 4H^+ \rightarrow Fe^{3+} + 2H_2O \qquad (3)$$

a reaction kinetically enhanced by the presence of anaerobic microorganisms like iron-oxidizing bacteria [14]. Bearing in mind the partial reactions (1)–(3), the global oxidation reaction is:

$$4FeS_2 + 15O_2 + 2H_2O \rightarrow 4Fe^{3+} + 4SO_4^{2-} + 4HSO_4^- \qquad (4)$$
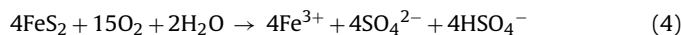
* Corresponding author. Tel.: +34 94 601 2707; fax: +34 94 601 3500.
** Co-Corresponding author.
E-mail addresses: juanmanuel.madariaga@ehu.es (J.M. Madariaga), felipeqma@yahoo.com.br (L.F.O. Silva).

where a highly buffered acid solution (pH $\approx$ 2) is formed being equimolar with the amount of dissolved Ferric ion released. In these conditions all the Ferric ion remains dissolved in the water solution.

While oxidative surface reactions on Fe sulphide minerals have been studied [9], far fewer studies have focused on the dissolution of other sulphide minerals. The direct oxidation of such cation divalent sulphides, like sphalerite

$$ZnS + 2O_2 \rightarrow Zn^{2+} + SO_4^{2-} \qquad (5)$$

does not lead to acidification. At low pH (<3), the oxidative dissolution of sphalerite can be catalyzed by abiotic Fe^{3+} reduction and subsequent oxidation of Fe^{2+} by *Thiobacillus ferrooxidans* [15]. If the Fe^{2+} is not completely reoxidized or if it is leached by the soil water, Fe^{3+}-mediated sphalerite oxidation results in a net acid release [16].

Dissolved cations and sulphate anions, released as acidic solutions from the oxidation of metal sulphides associated with coals, can interact among themselves (dissolved lead and sulphate can precipitate lead sulphate even in acidic solutions) or with the dissolved ions in waters (mainly bicarbonate) or the minerals in the river sediments (mainly carbonates) leading to the formation of secondary sulphate minerals and/or different metal oxides, (oxy)hydroxides or carbonates. These complex interactions must be thoroughly understood to assess potential risks for the environment and even to the human health.

This study investigated the nature of the coal mining residues (CMRs) and attempts to quantify the extent to which interaction has taken place or could take place between the coal or coalbearing strata and the surrounding environment, by using an accelerated weathering procedure based on the Fenton's reaction, i.e. using H_2O_2 as the oxidant to examine experimentally the oxidation of metal sulphide mineral phases associated with Brazilian coals.

The purpose is to evaluate the process of oxidation of the sulphides material in order to deduce the environmental fate of Fe, Ni, Cu, Pb, Mn, Zn, Co, Cd, H^+ and SO_4^{2-} in the Santa Catarina coal mining region. The results of such research are of great use in the design of prevention and remediation strategies for mine-affected regions.
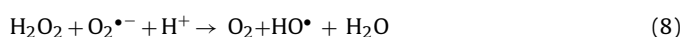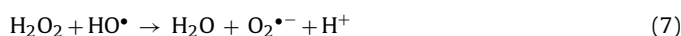
2. Background of the accelerated weathering by Fenton's reaction

Hydrogen peroxide (H_2O_2) has strong oxidizing properties and has been suggested as an appropriate chemical for clean desulphurization treatments of high-sulphur coals. It was determined to be effective in reducing >90% of the pyritic sulphur from high-sulphur coal [17–20].

The oxidation of redox-active ferrous ion (Fe^{2+}) by H_2O_2, known as the Fenton's reaction, results in the formation of ferric ion (Fe^{3+}) and hydroxyl ($HO^\bullet$) radicals consuming an equimolar amount of H^+ and hydroxyl (OH^-) ions:
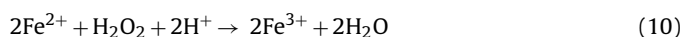
$$Fe^{2+} + H_2O_2 + H^+ \rightarrow Fe^{3+} + HO^\bullet + H_2O \qquad (6)$$
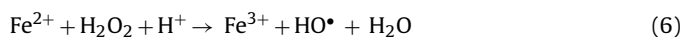
The Fenton reaction initiates a series of chain reactions, known as the Haber–Weiss cycle, in which H_2O_2 is consumed as follows:
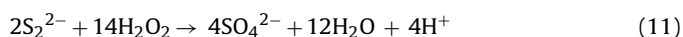
$$H_2O_2 + HO^\bullet \rightarrow H_2O + O_2^{\bullet-} + H^+ \qquad (7)$$

$$H_2O_2 + O_2^{\bullet-} + H^+ \rightarrow O_2 + HO^\bullet + H_2O \qquad (8)$$

while chain termination is expressed by the reaction:

$$Fe^{2+} + HO\cdot + H^+ \rightarrow Fe^{3+} + H_2O \qquad (9)$$

leading to the global oxidation in acid media:

$$2Fe^{2+} + H_2O_2 + 2H^+ \rightarrow 2Fe^{3+} + 2H_2O \qquad (10)$$

Disulphide anions can also be oxidized to sulphate by hydrogen peroxide, generating protons:

$$2S_2^{2-} + 14H_2O_2 \rightarrow 4SO_4^{2-} + 12H_2O + 4H^+ \qquad (11)$$

Pyrite oxidation by hydrogen peroxide may be represented by reaction:

$$2FeS_2 + 15H_2O_2 \rightarrow 2Fe^{3+} + 4SO_4^{2-} + 14H_2O + 2H^+ \qquad (12)$$
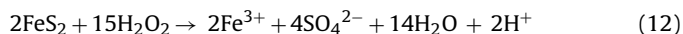
however, in order to understand the consequences of pyrite oxidation in geochemical processes and viable abatement of acid mine drainage, new data is needed to model the pyrite oxidation in the presence of dissolved metal ions, as some recent works have shown [18].

While the Fenton reaction, as represented by Eqs. (6)–(12), is a homogeneous reaction, the reaction can also proceed when ferrous iron is present as a solid. For example, [21] have shown that magnetite facilitates the conversion of H_2O_2 to $HO^\bullet$ via the Fenton reaction mechanism. Even Fe(III)-oxides and (oxy)hydroxides can facilitate the reaction albeit less effectively than magnetite [21,22]. For those authors, Fe(III)-oxide minerals may be reduced in the presence of H_2O_2 through the following reaction:

$$Fe^{III}(oxidemineral) + H_2O_2 \rightarrow Fe^{II}(oxidemineral) + (O_2^\bullet)^- + 2H^+ \qquad (13)$$
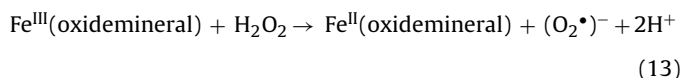
although other reaction mechanisms could be possible.

The aim of the work presented in this paper is to verify this possibility as well as the use of the Fenton's Reaction as an accelerated test for the weathering of pyrite, associated to coal (and/or the other sulphide minerals). Regardless of whether the Fenton reaction takes place in solution or on the surface, pyrite could readily reduce ferric iron; the reaction between dissolved ferric iron and pyrite has been studied extensively in the context of acid mine drainage [23].

3. Experimental

3.1. Study area

The South of Brazil, comprising the states of Santa Catarina and Rio Grande do Sul, has been known for its abundant and economically important coal beds since the beginning of the 20th century. While most of the coal reserves are found in the southernmost state of Rio Grande do Sul, the state of Santa Catarina boasts the greatest production [24–26].

When exposed to wind and rain, the rejects from coal beneficiation propitiate the development and growth of the bacteria *Thiobacillus ferrooxidans* and *Thiobacillus thiooxidans* speeding up the reactions of the pyrite oxidation and initiating a cycle that generates acid drainage bearing considerable pollution [3]. The oxidation of weather exposed sulphides in the tracts and basins of silts is produced by the action of O_2 and the Fe^{3+}, releasing soluble cations and dissolved sulphate. The sulphate minerals formed are easy to see as white precipitates on the blackish surface of the CMRs; those deposits only remain in solid form in conditions of easy evaporation. They are very soluble, show acid reaction and its formation implies important environmental risks, because the dissolved heavy metals are in a mobilizable and bioavailable form [3].

Both coal mining residues (CMRs), with and without white deposits on the surface, were selected to perform the study presented in this work.
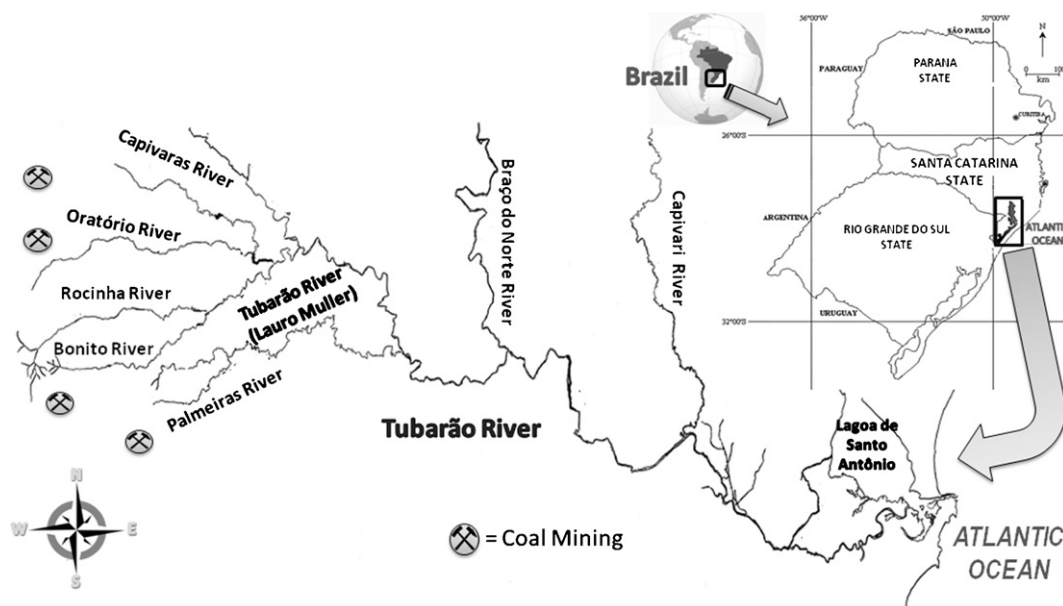
Fig. 1. Location of Santa Catarina state coal basin (Southern Brazil).

3.2. Coal mining residues samples

The 17 samples used for this study were obtained from Santa Catarina (Fig. 1). The samples were collected directly at source from open air hollows in the region of Lauro Muller city, which impacts in the hydrographic basin of the Tubarao River. The samples, gathered from different spots on the most recent stack in the same week, were stored in sample bags weighing between 20 and 25 kg. The samples, collected following either [27] and/or [28] procedures, were homogenized according to [29] norm D2797 and split into batches for the various analyses. Samples belong to two groups of materials:

a) *CMR-S*: Sediments originating from areas in contact with layers of coal, rich in carbonaceous substance (%C = 2.9–5.9) with variable levels of sulphur (%S = 0.2–3.2) and acid reaction.
b) *CMR-O*: Distinct sediments collected in the influence areas of the mines, but with low levels of carbonaceous matter and sulphur (%S < 0.1) and low acid reaction.

3.3. Analytical procedures for total metals contents from coal mining residues

All samples were acid digested following a two-step digestion method devised to retain volatile elements in coal dissolution [30]; this consisted of a HNO_3 hot extract followed by $HF:HNO_3:HClO_4$ acid digestion of the residue. The resulting solution was then analysed by Inductively Coupled Plasma Atomic-Emission Spectrometry (ICP-OES) for major trace elements and by Inductively Coupled Plasma Mass Spectrometry (ICP-MS) for additional trace elements. The digestion of the international reference materials (SARM-19) and blanks was also conducted following the same procedure to check the accuracy of the analytical and digestion methods. Uncertainties were estimated at <3% for most of the elements and around 10% for Cd, Mo and P. Mercury analyses were carried out directly on solid samples using LECO AMA 254 gold amalgam atomic absorption spectrometer.

3.4. Mineralogical analysis procedures

The occurrence of mineral species was investigated by means of Powder X-ray diffraction (XRD), environmental Scanning Electron Microscope (SEM) coupled with an energy dispersive X-ray microanalysis system (EDX) [31] and Transmission electron microscopy (TEM) for chemical analyses of individual particles.

Prior to TEM analysis different suspensions were selected, namely hexane, acetone, dichloromethane and methanol, as a function of the mineral considered in order to prevent possible mineralogical changes when a proper suspension is not used. The suspension consisted of 10 mL of each of the solvents mixed with 0.5 g of dried and sieved coal mining residue. The mixture was placed in an ultrasonic bath for 30 min. The suspension was stirred for ~1 min, pipetted onto lacycarbon films supported by Cu grids [2] and finally left to evaporate before the TEM analysis was performed [22].

Analytical electron microscopy using a Scanning Electron Microscopy (SEM) and transmission electron microscope (TEM) offers great advantages in both spatial resolution and reduced sample volume to perform the analysis. Studies by Hochella et al. [32] and Genovese and Mellini [33] have demonstrated the benefits of utilizing TEM in acid-mine drainage systems as it allows the analyst to see particles, even down to the nano-scale, as well as their associated chemistry and crystallography [4].

3.5. Oxidation by H_2O_2

Hydrogen peroxide is an eco-friendly, strong oxidant and effluents treated with it are more susceptible to biodegradation. Consequently, hydrogen peroxide in the presence of a catalyst is gaining importance for secondary or even primary treatment of industrial effluents, including sulphide-bearing wastewaters, to meet the desired discharge limit. In this work, a forced oxidation of the coal cleaning residues with hydrogen peroxide was performed as an accelerated weathering test to evaluate the mobilizable metallic fraction associated with sulphides and the release potential during oxidation.

All experiments were carried out batchwise in a mechanically agitated glass reactor. Previously, pretreated samples (powdered, sieved through 2-mm mesh and homogenized) were oven-dried

Table 1
Range of the elemental composition (mean value and confidence interval at 95% of significance), for trace element contents, of the CMRs distributed as CMR-S and CMR-O.

mg kg^{-1}	CMR-S	CMR-0	%	CMR-S	CMR-0
As	19.5(1.0)	8.3(0.5)	Al	10.23(0.52)	10.22(0.42)
B	9.8(0.6)	15.0(1.7)	Ba	0.12(0.01)	0,071(0.002)
Ba	538(24)	952(33)	Ca	0.53(0.21)	0.76(0.03)
Be	3.1(0.2)	4.6(0.1)	Fe	3.13(0.42)	2.94(0.17)
Bi	1.5(0.4)	0.91(0.04)	K	1.54(0.15)	1.57(0.04)
Cd	4.5(0.2)	1.3(0.2)	Mg	0.27(0.01)	0.40(0.02)
Co	5.4(0.2)	11.1(0.5)	Na	0.12(0.01)	0.28(0.01)
Cr	48(1)	53(1)	P	0.29(0.01)	0.020(0.003)
Cu	24(1)	25(2)	Ti	0.55(0.03)	0.46(0.09)
Ga	28(1)	27(1)			
Ge	3.8(0.2)	3.7(0.2)			
Hf	5.0(0.3)	5.4(0.4)			
La	37.0(0.2)	38(1)			
Li	89(4)	81(3)			
Mn	51(3)	235(11)			
Mo	32.8(1.3)	3.4(0.1)			
Ni	66(1)	19.2(0.8)			
Pb	71(2)	45(4)			
Sb	1.23(0.05)	1.03(0.17)			
Se	5.4(0.5)	5.3(0.2)			
Sn	57(4)	5.0(0.1)			
Sr	91(7)	242(66)			
Ta	5.1(0.2)	4.9(0.2)			
Th	31(1)	22.6(0.1)			
U	6.5(0.7)	9.4(0.5)			
V	92(2)	98(2)			
W	6.9(0.2)	7.0(0.3)			
Y	22(1)	24.4(0.7)			
Zn	46(2)	191(11)			
Zr	183(9)	200(11)			

at 45 °C for 24 h and then transferred to a desiccator. Powdered samples of 1 g were treated with 100 mL aqueous solution of 15% H_2O_2 (Merck, Germany, diluted with Milli-Q ultrapure water), previously adjusted to pH = 5.5, and kept in an isothermal shaker bath at 30 °C for 72 h. An aliquot of 10 mL was withdrawn at preset intervals (of 1, 2, 6, 24, 48 and 72 h) and immediately filtered. Leachates were collected, weighed and separated into two aliquots. Sulphate, nitrate, conductivity, Eh and pH were determined immediately after the collection in the first aliquot. The second aliquot was acidified with concentrated HCl to prevent precipitation reactions and the total contents of elements and S were determined by ICP OES.

The optimum time of oxidation was set at 72 h in line with the results by Urrutia et al. [34] that had observed the segment of the kinetic and of oxidation of the sulphides with H_2O_2 for 27 days, showing little or no variation after the first 72 h.

4. Results and discussion

4.1. Elemental content

Table 1 shows the average range of variation (confidence level at 95%) of the total elemental composition of each metal in the unchanged coal washing residues grouped according to the type of material and the sulphur content, CMR-S and CMR-O respectively. The pyrite difference in the samples seems to directly influence the concentrations of all the toxic elements, with a clear tendency to increase parallel to the sulphur content, except for Mn. These results are supported by other studies that investigated the origin and correlations of metals with different sulphides [35–37] and the geochemical mobility of metals [38,39].

A suggested explanation for the high concentrations of Pb and Zn is both elements' association with pyrite (galena and sphalerite respectively) in the coal from the Santa Catarina Basin, whereas

Cd may occur primarily as a replacement for Zn in the mineral sphalerite.

4.2. Mineralogical characterization

The major minerals in the coal mining residues studied (in decreasing order of significance) are quartz (Fig. 2A), kaolinite (Fig. 2C), pyrite (Fig. 2D) and calcite (Fig. 2F) according to the XRD, TEM and SEM/EDX investigations. Other minerals, such as illite (Fig. 2B), gypsum (Fig. 2E), hematite (Fig. 2G), dolomite, ankerite, chlorite, opal, feldspars, rutile, marcasite and melanterite, were also identified in the CMRs as minor and accessory species.

The principal oxide detected in the CMRs analysed was hematite (Fig. 2G), closely mixed with quartz, feldspar and rutile. The hematite probably reflects the oxidation of pyrite in the coal, as indicated by studies on American coals [5]. The formation of iron oxides and hydroxides is considered the driving force behind the geochemical cycling of metals and the dissolution of redox-sensitive metal oxides [40] or biomineralization products [41]. These oxides are surface active reservoirs that trap dissolved cations or anions by surface complexation and/or precipitation mechanisms [42].

Carbonate minerals are common in the CMRs samples studied. They are represented by calcite (Fig. 2F) and, to lesser extents, by dolomite and ankerite. Calcite is mostly associated with coal macerals and occurs in association with vitrinite and also in cell-filling form in inertinite in Genesee feed-coal [43].

Sulphide minerals consist of pyrite (Figs. 2D and 3A), marcasite, pyrrhotite, sphalerite (Fig. 3B) and galena (Fig. 3C). The composition of pyrite surface and the tendency of metal ions from aqueous solution to be adsorbed on them can, to a considerable extent, also influence the rate of oxidation. This is consistent with the fact that metals like Na, K, Ca, Mg, Al, Ni, Cu, Ag, Pb, Zn, Cd and As, are known to occur on the natural pyrite surface [44].

Pyrite is the main species promoting the sulphur oxidation in the coal mining residues samples studied. Pyrite weathering, the main process leading to acid mine drainage [13], results from a combination of oxidation and dissolution processes involving ferric ion and oxygen and from microbial activity [9]. Additionally, pyrite is an ubiquitous component in the environment and should thus be considered as a reservoir of reductants for oxidized species with environmental relevance, such as heavy metals. Pyrite is probably the most environmentally interesting mineral in the coal slagheaps, coal beneficiation and generated CMRs, because of its propensity to oxidize during weathering, producing sulphuric acid that can leach trace elements associated with the pyrite and other constituents in the coals [45].

4.3. Oxidation of the sulphides and mobilization of elements

For a long-term assessment of the mobility of heavy metals from CMRs, it is particularly important to obtain information about potential acid immission and internal acid formation in relation to the buffer capacity of the contaminated site and their environment [16]. Thus, the oxidation of CMRs by hydrogen peroxide can give such information especially if we consider the presence of other metals together with the pyrite phases.

In a forced oxidation experiment with H_2O_2 almost all total sulphur occurred in the form of sulphide and the sulphur of the SO_4^{2-} does not represent a significant percentage in the original samples. Experimental results show that the dominant sulphur products during oxidation of pyrite by H_2O_2 are aqueous sulphate, hydrated iron sulphates and elemental sulphur.

This was demonstrated by analysing the surface of the CMRs a few minutes after Fenton's reaction was started as the accelerated weathering procedure. As seen in Fig. 4, new small jarosite crystals
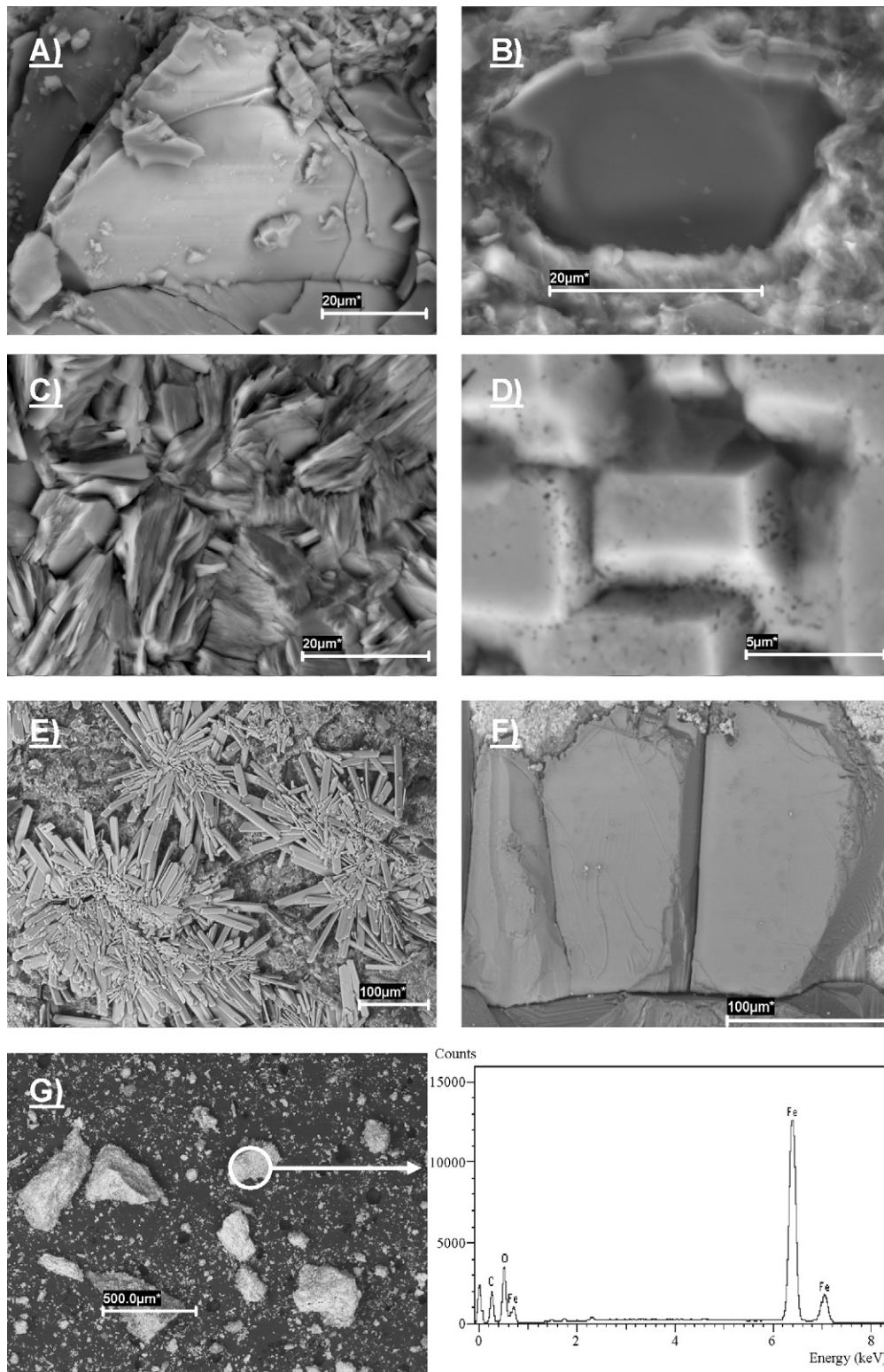
Fig. 2. The major minerals in the CMRs from Santa Catarina Coal Mining (SEM image): (A) quartz; (B) illite; (C) kaolinite; (D) typical cubic pyrite; (E) gypsum; (F) calcite; and (G) hematite (SEM/EDX).

were seen even after 3 min of the chemical attack, both on gypsum surfaces (Fig. 4A) or on K-feldespar (Fig. 4C). Gypsum and barite (Fig. 4B) can be considered secondary minerals formed after the oxidation of pyrite.

Pyrite, which under the same experimental conditions reacts with deoxygenated water (H_2O_2), did not show detectable sur-

face alteration and no dissolved sulphur species were identified in the supernatant solution, suggesting minimal reaction in the absence of H_2O_2. Given that water simply physisorbes molecularly to the pyrite surface [46], the presence of an active oxidizing species seems to be critical to initiate pyrite oxidation in an anoxic environment.
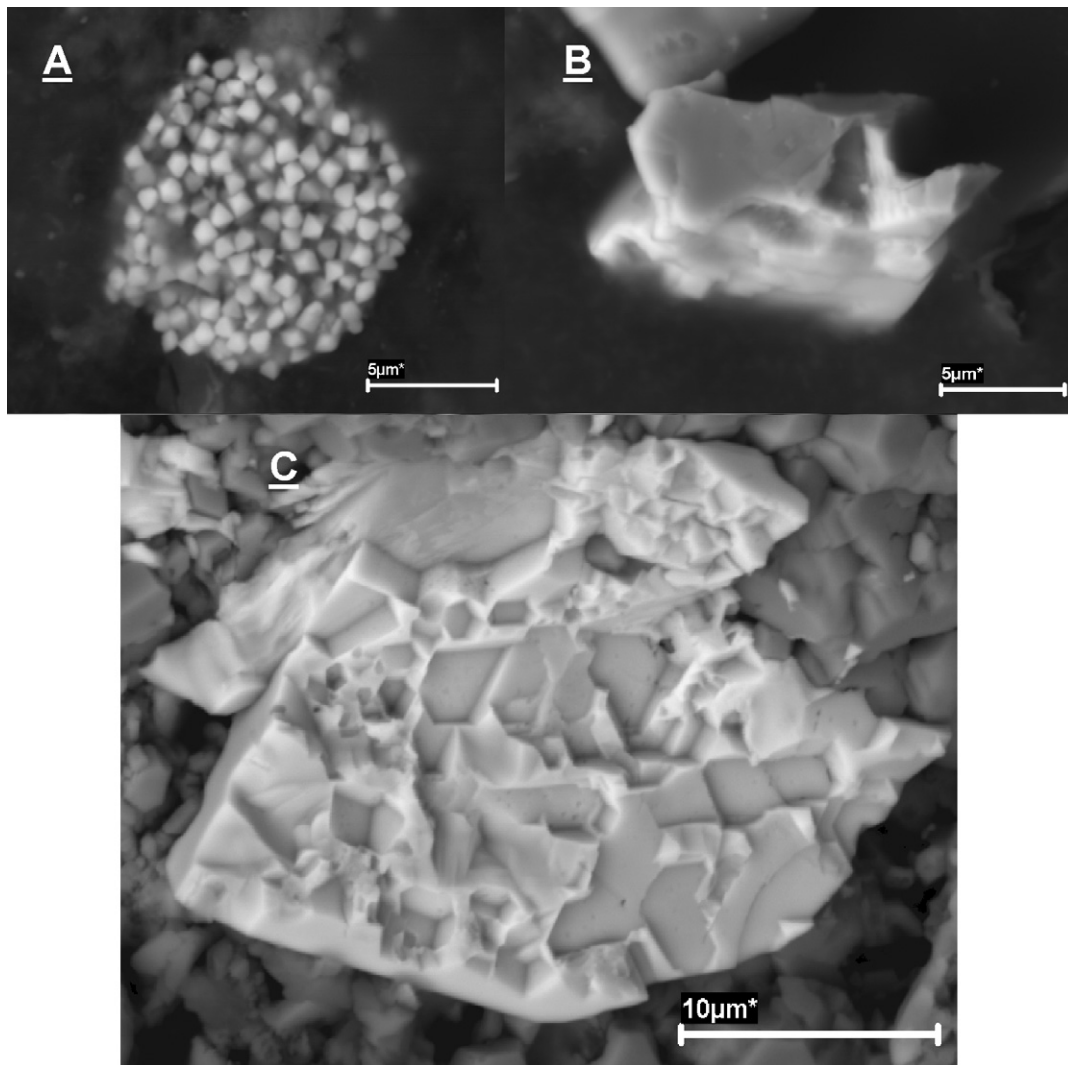
Fig. 3. SEM images of (A) pyrite framboids, perhaps the most common form of occurrence of syngenetic pyrite in coal and organic-rich shales; (B) sphalerite grains; and (C) galena fragment.

Pyrite oxidation appears to occur by direct reaction between HO• and the disulphide groups on the pyrite surface. Previous studies have shown that HO• could affect oxidation kinetics of intermediate sulphur species formed during stepwise oxidation of pyrite, such as sulphite [47], trithionate and tetratonate [48] and thiosulfate [49]. In solution, HO• can initiate a series of free radical chain reactions involving Fe^{2+} and H_2O_2, conforming to reactions (6)–(12), with the production of Fe^{3+}, H^+, and H_2O. Secondary pyrite oxidation reactions involving Fe^{3+} and O_2 are consistent with previously published studies of pyrite reactivity [10,50].

The maximum acidification produced by the complete oxidation of sulphide minerals in CRMs was evaluated. In all the analysed samples (Fig. 5A), the pH of the system reaches values between 2 and 3 when the sulphur content varies between 0.5 and 1.0%, and reaches values lower than 2 when sulphur content is greater than 1%. The release of soluble Fe follows a parallel trend to the percentage of S^- oxidised to SO_4^{2-}, but in many samples a lower concentration of dissolved total Fe was detected, as a function of the S content; this effect can be an indication of a fast precipitation of mineral phases of Fe, such as the detected freshly formed jarosite.

In order to confirm this hypothesis, a geochemical model was constructed following the methodology proposed elsewhere [51]. This type of chemical modelling has previously been used by the authors to explain the degradation of a mural painting due to water infiltrations containing ammonium nitrate [52], the transport of Arsenic from river waters to estuarine systems [53], the impact of NO_x from ship engines dissolving the facades of a Historical Palace House due to the formation of soluble nitrate compounds [54], the transformation of inorganic mineral pigments to other mineral phases due to atmospheric SO_2 impact [55] or organic oxalic acid excreted by microorganisms [56].

Fig. 5B shows the molar fraction diagram obtained when pyrite, in amount equivalent amount to 145 mM (in a carbonate–hydrogensulphide environment), is subjected to a continuous hydrogen peroxide attack, like in the experimental setup conditions used for samples 2–6. As seen the pyrite oxidation first promotes the appearance of sulphate in solution, to form the soluble Fe(II)–sulphate complex, as well as the precipitation of siderite. As the oxidation proceeds, the siderite fraction decreases while the soluble Fe(II)–sulphate complex increases until it reaches a state in which all the oxidised pyrite becomes the soluble Fe(II)–sulphate. In this step of the oxidation process, gypsum is formed by reaction of the freshly oxidised sulphate species and the calcium ions released by the acid attack in the calcite phase.

When all the pyrite has been oxidised, the added hydrogen peroxide starts oxidising Fe(II) to Fe(III). If sulphate ions are available in sufficient quantities, hydrogen–jarosite can be saturated but only if specific conditions are fulfilled.
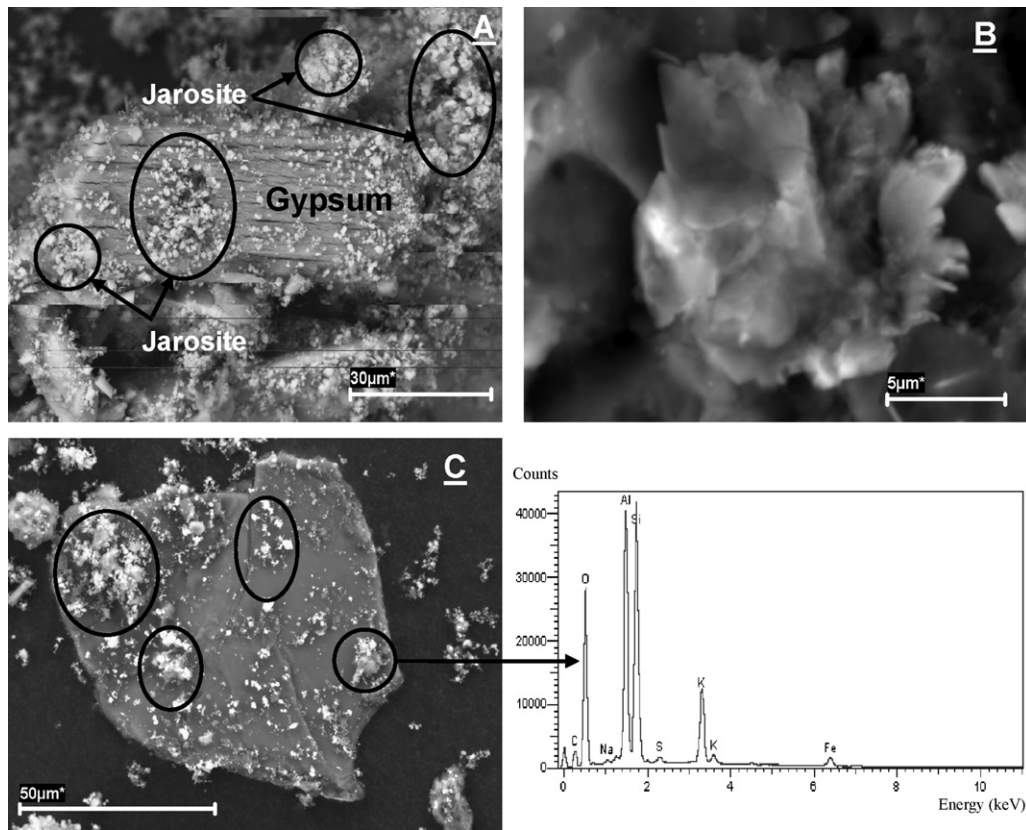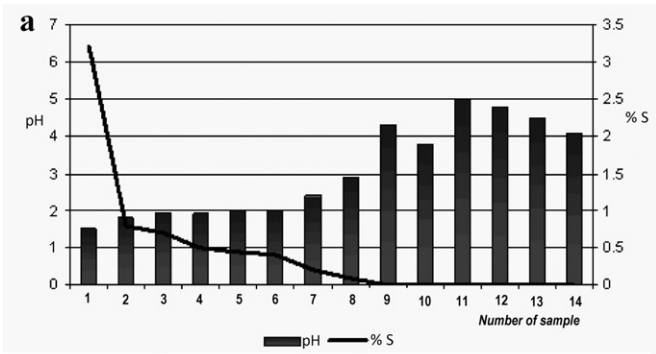
Fig. 4. SEM images (A) gypsum crystals in a massive association with new small jarosite crystals formed during the oxidative process by H_2O_2 (obtained after the first 3 min of the H_2O_2 oxidation); (B) barite; (C) K-feldspar in an association with small jarosite crystals (SEM/EDX).
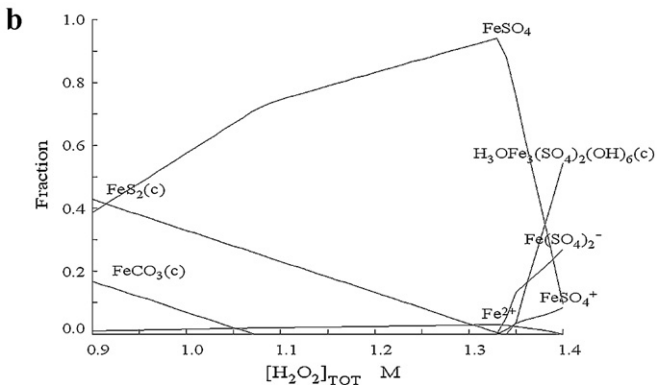

Fig. 5. (A) Variability of pH versus S concentration content in CMRs for some of the analysed samples; (B) theoretical modelling of pyrite oxidation as a function of the hydrogen peroxide addition in a carbonate beadrock.

The chemical modelling shows that carbonate is required in the near environment to neutralise the excess of hydrogen ions produced during the oxidation reaction. If that carbonate is not available, jarosite is not formed and the prediction gives hematite as the stable Fe(III) solid phase (we have experimentally detected several hematite crystals in all the analysed CMRs).

The second chemical condition required for hydrogen–jarosite to saturate is that sulphate must reach a given concentration in the solution around the CMR solid materials. The sulphate ions enter the system by two routes. In one, sulphate is released by the Fe(II)–sulphate complex when the Fe(II) is oxidised to Fe(III), breaking the stable sulphate complex. In the other process sulphate is released by the gypsum solid phase (gypsum is partially soluble in water) giving a solubility near to 1800 mg/L; these two sources of soluble sulphate ions give the high sulphate concentration required to saturate jarosite.

Predictions as to the chemical conditions resulting from the thermodynamic model (jarosite formation after gypsum precipitation) were made experimentally, as can be observed in Fig. 4B, where new jarosite crystals have formed on gypsum surfaces.

Few of the other metal sulphides produce so many hydrogen ions as the oxidation of pyrite. In our samples, the increase in %S is accompanied by a systematic increase in the total acidity (Fig. 5B). Thus, the principal sulphide compound in the CMRs must be pyrite because it is the compound promoting the greatest formation of soluble protons after its oxidation.

High sulphide oxidation rates were found in samples with low pH (<3), increasing the elements' mobilization into the medium. Our current results indicate that the efficiency of H_2O_2 treatment in partially oxidized CMRs depends on the proportions of Fe-oxides and sulphides present in the sample.
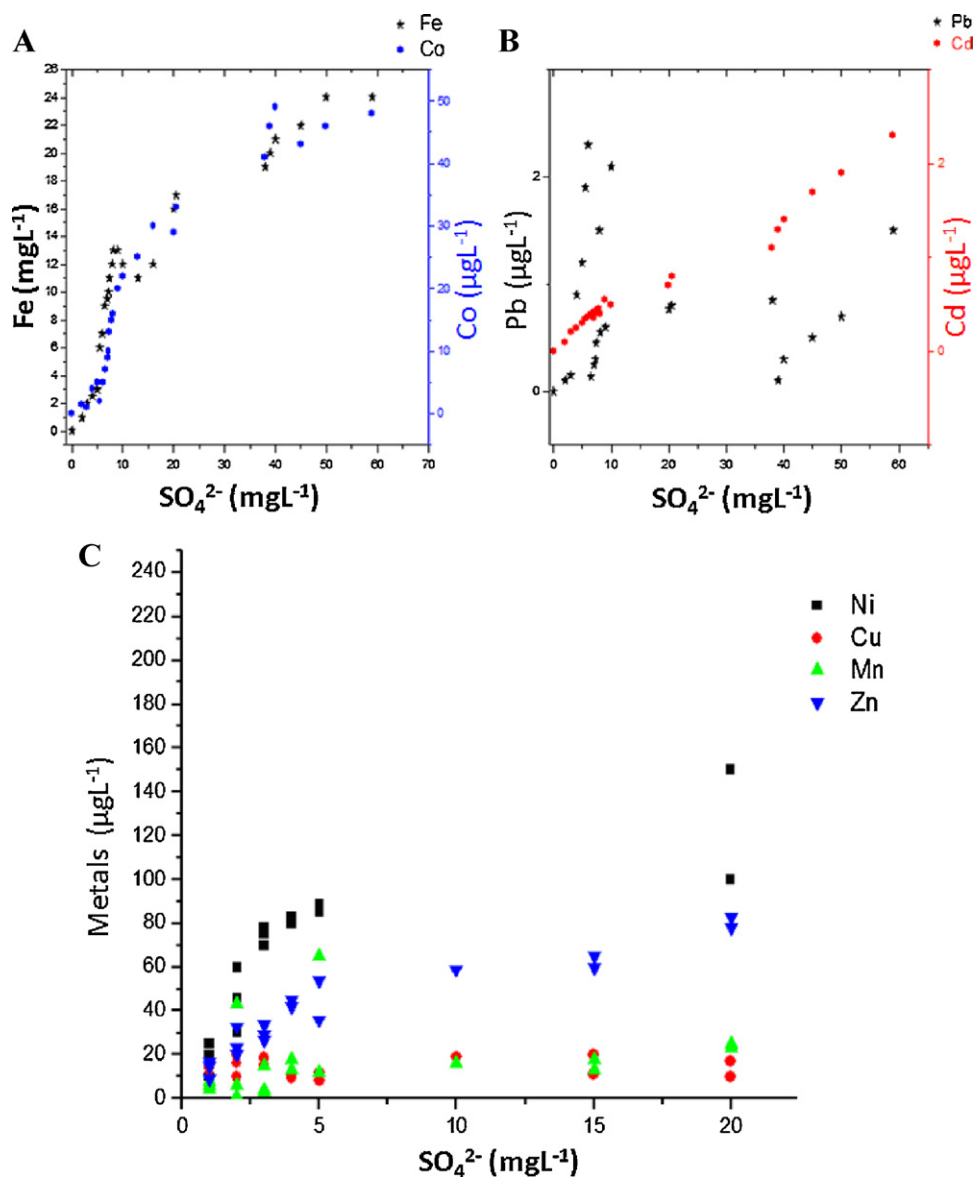
Fig. 6. Concentration of metals as a function of SO_4^{2-} concentrations during the oxidation of the CMRs with H_2O_2.

During the oxidation of the CMRs with hydrogen peroxide, the mobilized fraction of metals is mainly attributed to the association of metal sulphides with coals, like it is shown in Fig. 6.

The low Fe mobilization during the oxidation (see Fig. 6A) corresponds to a group of samples that liberated into the solution less than $8\,mg\,L^{-1}$ of SO_4^{2-}, which corresponds to the total oxidation of 0.2% of pyritic sulphur; this group of samples presents a dissolution pH slightly acidic (>4.0), thus the Fe is quickly immobilized and must be present in low concentration in solution (most part of the total Fe is as trivalent iron that precipitates as oxy-hydroxides at such pH values). The remaining samples (with a total content >1.3% of pyritic sulphur) displayed linear behaviour with the sulphate concentration, adjusting with the theoretical release of 2 mol of SO_4^{2-} and 1 mol of Fe per mol of oxidized pyrite (see reaction (12)). This behaviour can be explained by the acid pH promoted by the minerals phases having high pyrite concentration. As pyrite increases the amount of both, the free protons and the dissolved sulphate increase and, consequently the dissolved iron associated to pyrite. When the dissolved sulphate reaches a concentration

higher than $50\,mg\,L^{-1}$ part of the iron is precipitated as jarosite (see Fig. 5A) and the mobilized metal decreases to that theoretical 2:1 (sulphate:iron) ratio.

The Co presents practically the same trend like Fe (Fig. 6A), although its mobilization is much lower than iron, probably due to its mixed mode of occurrence in the CMR mineral and/or to its lower presence in the sulphide minerals.

The principal source of Cd clearly seems to be the sulphide phases displaying a mobilization pattern congruent with the release of sulphates into the dissolution (Fig. 6B). The predominance of Cd^{2+} in the oxidized samples, during the experiment with hydrogen peroxide, is evident from the slope of the linear behaviour of this heavy metal.

The Pb release rate into the dissolution is a poor in comparison with other common metal sulphides and shows great variations (Fig. 6B), not showing any relationship to the sulphate (or any other soluble species or element) concentrations, nor to the pH values. The simulation conducted under oxidizing conditions of galena (the most probable source of lead) shows the systematic precipitation

of lead sulphate and this could be the cause of the possible immobilization of the Pb liberated during the oxidation in almost all the samples, even at the lowest pH values.

The mobilization of Mn follows a linear trend parallel to the release of SO_4^{2-} (Fig. 6C), appearing clearly as a metal associated with the sulphide phases or dissolved Mn–carbonate species. It is important to highlight the high acidity in the oxidation of these samples, which favoured the mobilization of Mn because the precipitation of its Mn(III) or Mn(IV) oxide needs only pH ~ 4 and it is expected to continue mobilized for as long as the pH remains acidic (<3), but it would precipitate in a river course where the initial discharged solution, containing the dissolved manganese, is neutralised.

The mobility results for Ni (its mobility increases as the amount of oxidised sulphate increases, like it is shown in Fig. 6C) seems to be conditioned by the presence of different sulphides containing Ni like millerite (sulphides that contains variable ratios of Ni, As and Sn) and pyrrotite (iron sulphide that can contain even 3–5% of Ni). In the same way, Zn mobilization follows a co-linear trend, with the release of sulphates in all the types of materials (Fig. 6C), but the zinc solubility increases when the pH decreases values.

The Cu mobilization presents a nearly constant concentration independently of the range of sulphide concentration in the samples. The absence of any relationship between the released copper and the solubilised sulphate could be an indication of the formation of secondary copper sulphate precipitates that gives a constant dissolved copper concentration.

5. Conclusions

The accelerated weathering procedure based on Fenton's Reaction has shown the release of toxic metals from the sulphide fractions associated with coal residues. The use of SEM/EDX, TEM, XRD, ICP-MS and ICP OES analyses were conducted on various samples from the Santa Catarina coal region with the aim of improving the understanding of the mineralogy and geochemistry of CMRs. The measurements were conducted on the original materials as well as on the materials left after applying the accelerated oxidation by hydrogen peroxide.

Accordingly with the theoretical predictions by geochemical modelling, the experimental results demonstrate the effective oxidation of pyrite, as well as the other metal sulphides, by hydrogen peroxide within a short time period complete after 72 h. In terms of relative mobility (% of total metal released during the test), Cu, Co, Cd and Zn appear as metals of high mobility, liberating practically all total content. The released concentration of Ni and Mn increases as sulphate increases but a considerable concentration of both metals remains immobile in the solid phases. The Fe presents a relatively lower release, because it suffers processes of further immobilization after pyrite oxidation, even at lower pH values, due to secondary mineral precipitation, such as jarosite; this fact considerably limits its mobility. Finally, Pb presents a practically null mobility and it does not represent a risk of potential contamination even in samples with high sulphide concentrations due to the possible formation of insoluble lead sulphate.

These results demonstrate that in restoration practice the selective management of spoils can be considered to offer the best protection against contamination of surface and subsurface waters and is the method which should be applied in the future construction of dump facilities.

Acknowledgements

References

[1] I.P. Bortoluzzi, Universidad de Santiago de Compostela, Doctoral Thesis, Spain, 2003.

[2] R. Giere, M. Blackford, K. Smith, TEM study of PM2.5 emitted from coal and tire combustion in a thermal power station, Environ. Sci. Technol. 40 (2006) 6235–6240.

[3] L. Silva, M. Oliveira, K. da Boit, R. Finkelman, Characterization of Santa Catarina (Brazil) coal with respect to human health and environmental concerns, Environ. Geochem. Health 31 (2009) 475–485.

[4] L.F.O. Silva, T. Moreno, X. Querol, An introductory TEM study of Fe-nanominerals within coal fly ash, Sci. Total Environ. 407 (2009) 4972–4974.

[5] K.L. Pinetown, C.R. Ward, W.A. van der Westhuizen, Quantitative evaluation of minerals in coal deposits in the Witbank and Highveld Coalfields, and the potential impact on acid mine drainage, Int. J. Coal Geol. 70 (2007) 166–183.

[6] V.P. Evangelou, Pyrite Oxidation and Its Control, CRC Press, Boca Raton, FL, 1995.

[7] R.T. Lowson, Aqueous pyrite oxidation by molecular oxygen, Chem. Rev. 82 (1982) 461–497.

[8] G.W. Luther Iii, Pyrite oxidation and reduction: molecular orbital theory considerations, Geochim. Cosmochim. Acta 51 (1987) 3193–3199.

[9] J.D. Rimstidt, D.J. Vaughan, Pyrite oxidation: a state-of-the-art assessment of the reaction mechanism, Geochim. Cosmochim. Acta 67 (2003) 873–880.

[10] M.A. Williamson, J.D. Rimstidt, The kinetics and electrochemical rate-determining step of aqueous pyrite oxidation, Geochim. Cosmochim. Acta 58 (1994) 5443–5454.

[11] D.K. Nordstrom, C.N. Alpers, C.J. Ptacek, D.W. Blowes, Negative pH and extremely acidic mine waters from Iron Mountain, California, Environ. Sci. Technol. 34 (1999) 254–258.

[12] C.J. Ptacek, D.W. Blowes, J.L. Jambor, M.C. Moncur, M.R. Gunsinger, Long-term sulfide oxidation, acid neutralization and metal release processes in mine wastes, Geochim. Cosmochim. Acta 70 (2006) 506–1506.

[13] P.C. Singer, W. Stumm, Acidic mine drainage: the rate determining step, Science 167 (1970) 1121–1123.

[14] K. Sasaki, Raman study of the microbially mediated dissolution of pyrite by *Thiobacillus Ferrooxidans*, Can. Mineral. 35 (1997) 999–1008.

[15] O.J. Garcia, J.M. Bigham, O.H. Tuovinen, Sphalerite oxidation by *Thiobacillus ferrooxidans* and *Thiobacillus thiooxidans*, Can. J. Microbiol. 41 (1995) 578–584.

[16] N. Schuwirth, A. Voegelin, R. Kretzschmar, T. Hofmann, Vertical distribution and speciation of trace metals in weathering flotation residues of a zinc/lead sulfide mine, J. Environ. Qual. 36 (2007) 61–69.

[17] E. Ahnonkitpanit, P. Prasassarakich, Coal desulphurization in aqueous hydrogen peroxide, Fuel 68 (1989) 819–824.

[18] D. Borah, M.K. Baruah, I. Haque, Oxidation of high sulphur coal. Part 2. Desulphurisation of organic sulphur by hydrogen peroxide in presence of metal ions, Fuel 80 (2001) 1475–1488.

[19] M. Gürü, B. V. Sariöz, C. Cakanyildirim, Oxidative desulfurization of tufanbeyli coal by hydrogen peroxide solution. Energy sources. Part A: recovery, utilization, and environmental effects 30 (2008) 981–987.

[20] S. Mukherjee, S.K. Srivastava, Kinetics and energetics of high-sulfur northeastern India coal desulfurization using acidic hydrogen peroxide, Energy Fuels 18 (2004) 1764–1769.

[21] R.J. Watts, M.D. Udell, S.H. Kong, S.W. Leung, Fenton-like soil remediation catalyzed by naturally occurring iron minerals, Environ. Eng. Sci. 16 (1999) 93–103.

[22] W.P. Kwan, B.M. Voelker, Rates of hydroxyl radical generation and organic compound oxidation in mineral-catalyzed Fenton-like systems, Environ. Sci. Technol. 37 (2003) 1150–1158.

[23] M.J. Borda, D.R. Strongin, M.A. Schoonen, A vibrational spectroscopic study of the oxidation of pyrite by molecular oxygen, Geochim. Cosmochim. Acta 68 (2004) 1807–1813.

[24] DNPM, Informativo Anual da Indústria Carbonífera, 1996, 89 p.

[25] SIECESC, http://siecesc.com.br/ (acessed 25.06.08).

[26] ABCM, http://www.carvaomineral.com.br/abcm/ingles.asp (accessed 25.06.08).

[27] ABNT (Associação Brasileira de Normas Técnicas), Amostragem de carvão bruto e ou beneficiado. NBR 8291, Associação Brasileira de Normas Técnicas, Rio de Janeiro, 1983.

[28] American Society for Testing and Materials (ASTM), Standard test methods for collection of a gross sample of coal (D2234-89), in: Annual Book of ASTM Standards: Gaseous Fuels; Coal and Coke, v 5.05, American Society for Testing and Materials, West Conshohocken, PA, 1996, pp. 236–247.

[29] American Society for Testing and Materials (ASTM), ASTM, Annual Book of ASTM Standards, Section 5, Petroleum Products, Lubricants and Fossil Fuels, Volume 05.05 Gaseous Fuels, Coal and Coke, D 2797: Standard Practice for Preparing Coal Samples for Microscopical Analysis by Reflected Light, 1991, pp. 308–310.

[30] X. Querol, A. Alastuey, A. Lopez-Soler, F. Plana, J.L. Fernandez-Turiel, R. Zeng, W. Xu, X. Zhuang, B. Spiro, Geological controls on the mineral matter and trace elements of coals from the Fuxin basin, Liaoning Province, northeast China, Int. J. Coal Geol. 34 (1997) 89–109.

[31] X. Querol, M. Izquierdo, E. Monfort, E. Alvarez, O. Font, T. Moreno, A. Alastuey, X. Zhuang, W. Lu, Y. Wang, Environmental characterization of burnt coal gangue banks at Yangquan, Shanxi Province, China, Int. J. Coal Geol. 75 (2008) 93–104.

[32] M.F. Hochella, J.N. Moore, U. Golla, A. Putnis, A TEM study of samples from acid mine drainage systems: metal-mineral association with implications for transport, Geochim. Cosmochim. Acta 63 (1999) 3395–3406.

[33] A. Genovese, M. Mellini, Ferrihydrite flocs, native copper nanocrystals and spontaneous remediation in the Fosso dei Noni stream, Tuscany, Italy, Appl. Geochem. 22 (2007) 1439–1450.

[34] M.J. Urrutia, E. Grana, Y.F. Garcia-Rodeja Macias, Procesos de oxidación de pirita en medios superficiales: potencial acidificante e interés para la recuperación de suelos de mina, Cuad. Lab. Xeol. Laxe 11 (1987) 131–145.

[35] B.C. Bostick, S. Fendorf, Arsenite sorption on troilite (FeS) and pyrite (FeS$_2$), Geochim. Cosmochim. Acta 67 (2003) 909–921.

[36] O. Dellwig, M.E. Böttcher, M. Lipinski, H.-J. Brumsack, Trace metals in Holocene coastal peats and their relation to pyrite formation (NW Germany), Chem. Geol. 182 (2002) 423–442.

[37] M. Schoonen, Mechanisms of Sedimentary Pyrite Formation, 379, Geological Society of América, 2004, pp. 117–134, special paper.

[38] A. Alastuey, A. García-Sánchez, F. López, X. Querol, Evolution of pyrite mud weathering and mobility of heavy metals in the Guadiamar valley after the Aznalcóllar spill, south-west Spain, Sci. Total Environ. 242 (1999) 41–55.

[39] H. Ernstberger, W. Davison, H. Zhang, A. Tye, S. Young, Measurement and dynamic modeling of trace metal mobilization in soils using DGT and DIFS, Environ. Sci. Technol. 36 (2002) 349–354.

[40] J. Ha, T. Hyun Yoon, Y. Wang, C.B. Musgrave, J.G.E. Brown, Adsorption of organic matter at mineral/water interfaces: 7. ATR-FTIR and quantum chemical study of lactate interactions with hematite nanoparticles, Langmuir 24 (2008) 6683–6692.

[41] J.F. Banfield, S.A. Welch, H. Zhang, T.T. Ebert, R.L. Penn, Aggregation-based crystal growth and microstructure development in natural iron oxyhydroxide biomineralization products, Science 289 (2000) 751–754.

[42] M.A. Olazabal, N.P. Nikolaidis, S.A. Suib, J.M. Madariaga, Precipitation equilibria of the chromium(VI)/iron(III) system and spectrospcopic characterization of the precipitates, Environ. Sci. Technol. 31 (1997) 2898–2902.

[43] F. Goodarzi, Mineralogy, elemental composition and modes of occurrence of elements in Canadian feed-coals, Fuel 81 (2002) 1199–1213.

[44] T.A. Al, D.W. Blowes, C.J. Martin, L.J. Cabri, J.L. Jambor, Aqueous geochemistry and analysis of pyrite surfaces in sulfide-rich mine tailings, Geochim. Cosmochim. Acta 61 (1997) 2353–2366.

[45] G. Liu, P. Yang, Z. Peng, C.-L. Chou, Petrographic and geochemical contrasts and environmentally significant trace elements in marine-influenced coal seams, Yanzhou mining area, China, J. Asian Earth Sci. 23 (2004) 491–506.

[46] K.M. Rosso, U. Becker, M.F.J. Hochella, The interaction of pyrite surfaces with O$_2$ and H$_2$O: fundamental oxidation mechanisms, Am. Miner. 84 (1999) 1549–1561.

[47] A.N. Ermakov, G.A. Poskrebyshev, A.P. Purmal, Sulfite oxidation: the state-of-the-art of the problem, Kinet. Catal. 38 (1997) 295–308.

[48] G.K. Druschel, R.J. Hamers, G.W. Luther, J.F. Banfield, Kinetics and mechanism of trithionate and tetrathionate oxidation at low pH by hydroxyl radicals, Aqueous Geochem. 9 (2004) 145–164.

[49] M. Schöneshöfer, Pulsradiolytische untersuchungüber das S$_4$O$_3^-$ radikal als wischenprodukt der thiosulfatoxidation und tetrathionatreduktion, Int. J. Radiat. Phys. Chem. 5 (1973) 375–386.

[50] G. Kameia, H. Ohmotob, The kinetics of reactions between pyrite and O$_2$-bearing water revealed from in situ monitoring of DO, Eh and pH in a closed system, Geochim. Cosmochim. Acta 64 (2000) 2585–2601.

[51] J.C. Raposo, J. Sanz, G. Borge, M.A. Olazabal, J.M. Madariaga, Development of a modified bromley's methodology (MBM) for the estimation of ionic media effects on solution equilibria. Part 3: application to the construction of thermodynamic models, Fluid Phase Equilib. 155 (1999) 1–19.

[52] M. Pérez-Alonso, K. Castro, M. Álvarez, J.M. Madariaga, Scientific analysis versus restorer's expertise for diagnosis prior to a restoration process: the case of Santa Maria Church (Hermo, Asturias, North of Spain), Anal. Chim. Acta 524 (2004) 379–389.

[53] J.C. Raposo, O. Zuloaga, J. Sanz, U. Villanueva, P. Crea, N. Etxebarria, M.A. Olazabal, J.M. Madariaga, Analytical and thermodynamical approach to understand the mobility/retention of arsenic species from the river to the estuary. The Bilbao case study, Mar. Chem. 99 (2006) 42–51.

[54] I. Martínez-Arkarazo, M. Angulo, L. Bartolomé, N. Etxebarria, M.A. Olazabal, J.M. Madariaga, An integrated analytical approach to diagnose the conservation state of building materials of a palace house in the metropolitan Bilbao (Basque Country, North of Spain), Anal. Chim. Acta 584 (2007) 350–359.

[55] K. Castro, M. Pérez-Alonso, M. Rodríguez-Laso, N. Etxebarria, J. Madariaga, Non-invasive and non-destructive micro-XRF and micro-Raman analysis of a decorative wallpaper from the beginning of the 19th century, Anal. Bioanal. Chem. 387 (2007) 847–860.

[56] K. Castro, A. Sarmiento, I. Martínez-Arkarazo, J.M. Madariaga, L.A. Fernández, Green copper pigments biodegradation in cultural heritage: from malachite to moolooite, thermodynamic modeling, X-ray fluorescence, and raman evidence, Anal. Chem. 80 (2008) 4103–4110.